The Optical Activity of the Pyridine Chromophore: MO Analysis of the Circular Dichroism Spectrum of 5α-Cholest-2-eno[3,2-*b*]pyridine

By **Serafino Gladiali**, Istituto di Chimica Applicata, Università di Sassari, Sassari, Italy
Giovanni Gottarelli * and **Bruno Samorì**, Istituto di Chimica degli Intermedi, Università di Bologna, Viale Risorgimento 4, Bologna, Italy
Paolo Palmieri,* Istituto di Chimica Fisica e Spettroscopia, Università di Bologna, Viale Risorgimento 4, Bologna, Italy

5α-Cholest-2-eno[3,2-*b*]pyridine (III), a chiral molecule containing the pyridine chromophore, was synthesized, and its c.d. spectrum measured between 195 and 300 nm. An *ab initio* computation of the optical activity was carried out on 5,6,7,8-tetrahydroquinoline, which has *P* chirality, and which was considered as the most important fragment in determining the optical activity of (III). Good agreement was found between the calculated values and the experimental c.d. spectrum of (III) for all accessible transitions. The low energy $n \longrightarrow \pi^*$ is red-shifted relative to the first $\pi \longrightarrow \pi^*$ transition and no crossing of the two transitions occurs. No substantial contribution to the optical activity is given by the $n \longrightarrow \pi^*$ transition at higher energy. The contributions of a one-electron mechanism to the optical activity of the $n \longrightarrow \pi^*$ and first $\pi \longrightarrow \pi^*$ transitions are briefly discussed.

In connection with previous work on optically active pyridines,[1-3] a rigid molecule containing the pyridine chromophore was needed to help characterize further the lower electronic excited states of the pyridyl chromophore

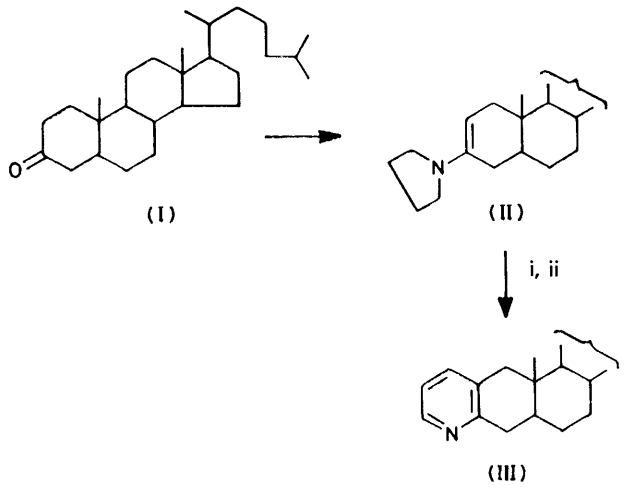

(I) (II) (III)

Scheme Regents: i, $H_2C{=}CHCHO$; ii, NH_2OH

and to clarify the relationships between optical activity and molecular structure for these systems; until now discussion on these points was based on experimental results obtained from conformationally labile molecules.[1,3-6] The presence of several possible conformations is a serious source of ambiguity in the interpretation of the various c.d. bands observed experimentally as these could originate from different conformers and not from different electronic transitions. Furthermore, the recent success obtained in non-empirical calculations of the optical activity of small ring derivatives stimulated us to extend the method to larger molecules of biological interest. For this purpose, it is of particular importance to select the parts of a complex molecule which play a major role in determining the c.d. spectra; the calculations are in this way reduced to accessible dimensions.

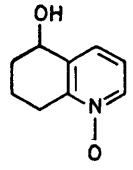

(IV)

RESULTS AND DISCUSSION

5α-Cholest-2-eno[3,2-*b*]pyridine (III) was prepared in three steps starting from 5α-cholestan-3-one (I) following the procedure depicted in the Scheme (see Experimental section). In (III) ring A of the cholestane moiety should

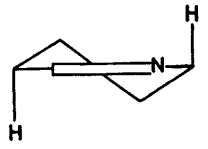

P—helicity

adopt a tetralin-like half-chair conformation, similar to 5-hydroxy-5,6,7,8-tetrahydroquinoline 1-oxide (IV) the structure of which was recently determined by the *X*-ray diffraction method.[7] This conformation does not cause severe strain in the steroidal skeleton which assures sufficient rigidity in the system; in particular no chair inversion of ring A, which in (III) has *P* chirality, can occur.†

Following Snatzke and his co-workers,[8] the chirality of the steroidal ring A (*P* or *M*), should be the principal factor in determining the sign of the c.d. spectra of the accessible aromatic transitions. This hypothesis was experimentally verified for several aromatic derivatives and was adopted here in order to simplify the calculations. The absorption and c.d. of (III) are reported in Figure 1: three transitions at *ca.* 282, 265, and 210 nm

† 5-Hydroxy-5,6,7,8-tetrahydroquinoline [1,5] was not considered as a suitable model as its conformation is not fixed and chair inversion can easily occur; the two conformations are almost certainly present in solution and their relative amount is unknown.

are clearly distinguishable in the c.d. spectrum of (III). The low temperature c.d. spectrum does not show relevant changes with respect to that at room temperature. In particular, the small negative band at *ca.* 282 nm is always present and more intense, and this seems to exclude the hypothesis of a hot band. No detectable c.d. maxima are present in the region of *ca.* 240 nm, contrary to what was found for conformationally mobile systems containing the pyridine chromophore.[1,3,4] The c.d. spectrum recorded in glacial acetic acid solution does not show the negative transition at 282 nm any more.

The absorption spectrum of (III) is very similar to that of pyridine. The bands at *ca.* 260 and 210 nm, which correspond to the $A_1 \longrightarrow B_2$ and $A_1 \longrightarrow A_1$ transitions of pyridine respectively, show corresponding maxima in the c.d. spectrum.

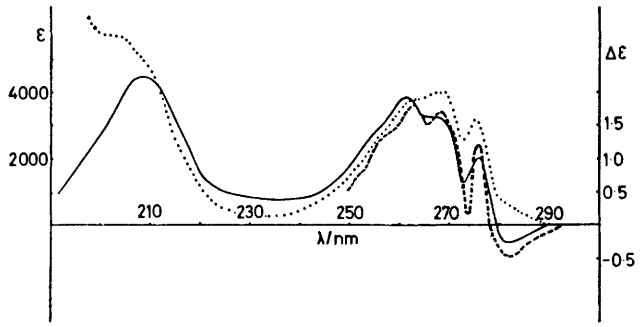

FIGURE 1 The absorption spectrum (· · · ·) and the c.d. spectrum at room temperature in cyclohexane (——) and at −160° in methylcyclohexane–isopentane (– – – –) of 5α-cholest-2-eno-[3,2-*b*]pyridine (III). The rotational strengths are −0.8, +3.6, and +3.5 × 10^{-40} c.g.s.u. from low to high energy

Excited States and Rotational Strengths from MO Theory.—The highest occupied and the lowest unoccupied MOs of the pyridine chromophore are essentially benzene e_{1g} and e_{2u} MOs. With respect to benzene, the main difference is represented by the lone pair orbital on the nitrogen atom, the orbital energy of which was computed to be slightly below the two highest occupied MOs. Actual computations of the MO expressions have been performed by an *ab initio* SCF treatment based on STO/3G [9] atomic orbitals. These are displayed in Figure 2, together with the computed orbital energies.

One Configurational Description of the Lowest n ⟶ π* *States and Two Configurational Descriptions of the Lowest* π ⟶ π* *States.*—The one-electron excitations, which are most likely to contribute to the lowest excited states, are classified into $n \longrightarrow \pi^*$ excitations [(5,8) and (5,9)] and $\pi \longrightarrow \pi^*$ transitions [(7,8), (7,9), (6,8), and (6,9)]. Actual values of the one-electron electric and magnetic transition dipoles, computed from the MO expressions, are listed in Table 1. As in benzene, the lowest $\pi \longrightarrow \pi^*$ states are represented, to a first level of approximation,

$$\begin{aligned} {}^1L_b &\cong 0.7717(7,8) + 0.6360(6,9) \\ {}^1L_a &\cong 0.7293(7,9) - 0.6842(6,8) \end{aligned} \qquad (1)$$

as linear combinations of the two degenerate configurations with identical local symmetry in the pyridine chromophore. Distortion of the molecular symmetry with respect to D_{6h} has a first-order effect on the linear coefficients of the degenerate $\pi \longrightarrow \pi^*$ configurations in the expansions (1), thus determining the dominant components of the electric ($\vec{\mu}$) and magnetic ($\vec{m}$) transition moments to the ${}^1L_b$ (μ_y, m_x) and ${}^1L_a$ states (μ_z). All remaining components are related to second and higher order effects. Of the two $n \longrightarrow \pi^*$ configurations, the (5,8) is to zero order electrically (μ_x) and magnetically (m_y) allowed, while the (5,9) transition has a

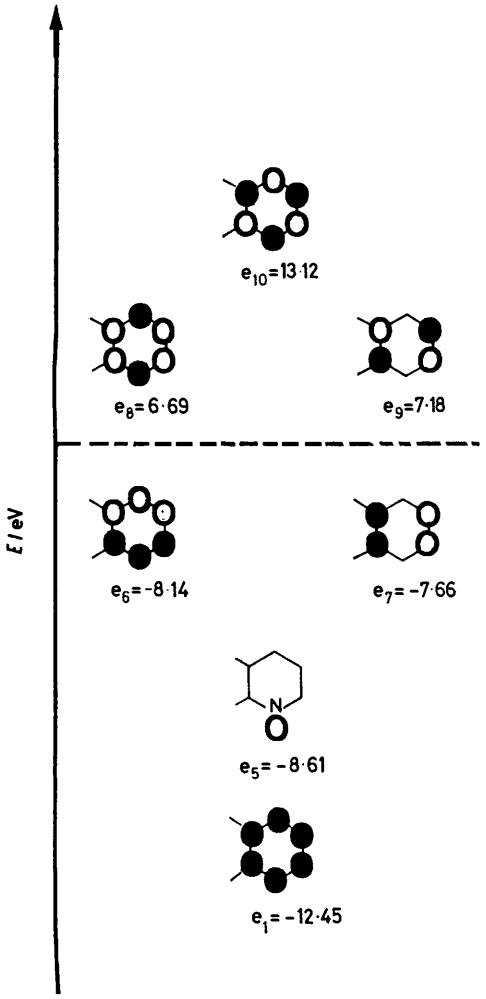

FIGURE 2 Simplified representation and energies of MOs of 5,6,7,8-tetrahydroquinoline. Orbitals (2)—(4) not represented in the Figure are the highest occupied σ MOs

vanishing electric dipole and a very small magnetic dipole, since it arises from very small two-centre contributions (see Figure 2). Therefore, the c.d. spectrum of 5,6,7,8-tetrahydroquinoline is expected to be dominated at low energy by one $n \longrightarrow \pi^*$ and two $\pi \longrightarrow \pi^*$ (${}^1L_a$ and ${}^1L_b$) states.

The electric and magnetic transitions dipoles and the rotational strengths for the lowest $n \longrightarrow \pi^*$ and $\pi \longrightarrow \pi^*$ states appropriate to this description are easily obtained from Table 1 and are listed in Table 2.

The energy sequence of the states is computed as $n \longrightarrow \pi^*$ (5,8) < ${}^1L_b$ < $n \longrightarrow \pi^*$ (5,9) < ${}^1L_a$ and there-

fore the c.d. spectrum should exhibit in the present description a positive band at low energy, followed by a negative band in contrast with the recorded spectrum.

TABLE 1

Electric $\vec{\mu}$ (10^{-2} a.u.) and magnetic $\vec{m}$ ($10^{-2}i$ a.u.) for the lowest $n \longrightarrow \pi^*$ and $\pi \longrightarrow \pi^*$ one electron excitations. Vector components are along the pseudosymmetry axes of the pyridine ring. The electric dipole components are computed in the dipole velocity representation

One electron excitation	Local symmetry	Axes	$\vec{\mu}$	$\vec{m}$
(5,8)	B_1	z	0.310	−4.006
		y	0.158	62.841
		x	−23.947	−0.674
(5,9)	A_2	z	1.519	−3.049
		y	1.005	0.184
		x	−2.684	−2.241
(5,10)	B_1	z	−0.787	−2.278
		y	+4.016	95.804
		x	−7.249	4.973
(7,8)	B_2	z	1.767	−0.021
		y	71.556	−1.866
		x	0.547	−4.865
(6.9)	B_2	z	−0.007	0.758
		y	−76.719	1.558
		x	0.164	1.318
(7,9)	A_1	z	−65.303	−2.544
		y	−0.405	−0.319
		x	−0.787	−0.488
(6,8)	A_1	z	−57.392	1.228
		y	0.219	0.912
		x	0.573	−5.891

n–^1L_b and ^1L_a–^1L_b Interactions and Relations with One-electron Theories of Optical Activity.—An improvement to the previous description is obtained by taking into account the small interaction energy term among the

TABLE 2

Electric $\vec{\mu}$ (10^{-2} a.u.) and magnetic $\vec{m}$ ($10^{-2}i$ a.u.) transition dipoles and rotational strengths R (10^{-39} c.g.s.) for the lowest $n \longrightarrow \pi^*$ and $\pi \longrightarrow \pi^*$ transitions. Approximate excited state wavefunctions given by equation (1)

State and local symmetry	Axes	$\vec{\mu}$	$\vec{m}$	R
$n \longrightarrow \pi^*$ (B_1)	z	0.438	−5.665	
	y	0.225	88.871	1.174
	x	−33.866	−0.953	
L_b (B_2)	z	1.922	0.658	
	y	9.093	−0.634	−0.179
	x	0.743	−4.124	
$n \longrightarrow \pi^*$ (A_2)	z	2.148	−4.312	
	y	1.421	0.260	−0.001
	x	−2.796	−3.169	
L_a (A_1)	z	−11.789	−3.811	
	y	−0.629	−1.212	0.910
	x	−1.365	5.917	

lowest $n \longrightarrow \pi^*$ and $\pi \longrightarrow \pi^*$ states. By perturbation theory, the approximate description for the $n \longrightarrow \pi^*$ state is obtained [equation (2)] with the energy difference defined as $\Delta E = E(5,8) - E(^1L_b)$. In one-electron theories[10] of the optical activity, the total Hamiltonian in equation (2) is substituted by an effective one-electron potential V associated with the incompletely shielded

$$n \longrightarrow \pi^*(B_1) = (5,8) + \langle ^1L_b|\mathscr{H}|5,8\rangle ^1L_b/\Delta E \qquad (2)$$

nuclear charges of the dissymmetric molecule environment of the pyridine chromophore. The matrix element may be then expanded into one-electron contributions [approximation (3)] where the interaction of the $n \longrightarrow \pi^*$

$$n \longrightarrow \pi^* \cong (5,8) + \sqrt{2}\langle 7|V|5\rangle ^1L_b/\Delta E \qquad (3)$$

and ^1L_b states is shown to proceed *via* mixing of the lone pair MO (5) with the benzene MO (7). In other words the $n \longrightarrow \pi^*$ excitation is followed by increased mixing of the occupied n and π orbitals.

The sign of the matrix element in equations (2) and (3) can be approximately predicted by considering the dominant contribution to V as given by the dissymmetric 7-methylene group (Figure 3). The positive potential associated with the incompletely screened nuclear charge of this group interacts repulsively with the overlap charge density of orbitals (5) and (7) having the phases depicted in Figure 3. Therefore the signs of the matrix

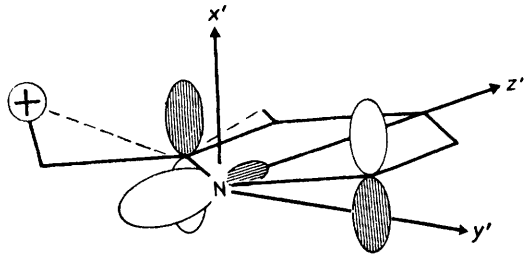

FIGURE 3 Representation of the interaction between orbitals (5) and (7) under the influence of the dissymmetric 7-methylene group in (*P*)-5,6,7,8-tetrahydroquinoline. For the orbital phases depicted, the interaction energy with the incompletely screened nuclear charge at C-7 is repulsive (positive). x', y', and z' are the axes of the local reference system centred at nitrogen

elements in equation (3) is expected to follow a quadrant rule. The signs of the rotational strength caused by this contribution are negative and positive for the $n \longrightarrow \pi^*$ and ^1L_b transitions respectively. The importance of these contributions will obviously increase with the lowering of the energy separation between the two transitions.

Exact evaluation of the matrix elements and of the energy difference in equation (2) gives equation (4) for the n–π^* state in qualitative agreement with the approxi-

$$n \longrightarrow \pi^* \cong 0.999(5,8) - 0.017\ ^1L_b \qquad (4)$$

mate theory. Similarly, the approximate expressions for the ^1L_a and ^1L_b states are obtained by considering the ^1L_a,^1L_b and ^1L_b,$n \longrightarrow \pi^*$ interactions [approximation (4′)].

$$^1L_b \cong 0.0169(5,8) + 0.9884\ ^1L_b + 0.1511\ ^1L_a$$
$$^1L_a \cong -0.1511\ ^1L_b + 0.9885\ ^1L_a \qquad (4')$$

As expected from the local symmetry of the two states, although energetically important, the ^1L_a,^1L_b interaction

does not modify the sign and the absolute values of the rotational strengths computed with equations (1). The $n \longrightarrow \pi^*$–^1L_b interaction produces a sign reversal of the ^1L_b transition magnetic moment and rotational strength,

TABLE 3

Electric $\vec{\mu}$ (10^{-2} a.u.) and magnetic $\vec{m}$ ($10^{-2}i$ a.u.) transition dipoles and rotational strengths R (10^{-39} c.g.s.) for the lowest $n \longrightarrow \pi^*$ and $\pi \longrightarrow \pi^*$ states. Approximate excited state wavefunctions given by equations (2) and (4).

State and local symmetry	Axes	$\vec{\mu}$	$\vec{m}$	
$n \longrightarrow \pi^*$ (B_1)	z	0.442	−5.666	
	y	0.051	88.872	0.764
	x	−33.872	−0.897	
$\pi \longrightarrow \pi^*$ (L_b)	z	−0.221	−0.020	
	y	8.918	0.689	0.146
	x	−0.008	−3.307	
$\pi \longrightarrow \pi^*$ (L_a)	z	−11.851	−3.867	
	y	−1.766	−1.103	0.930
	x	−1.438	5.760	

which is due to the large magnetic moment (m_y) of the $n \longrightarrow \pi^*$ transition (Table 3).

A sign reversal is not observed for the $n \longrightarrow \pi^*$ transition (5,8), the rotational strength of which is still dominated by the x components of the electric and magnetic transition dipoles.

CI Description.—All remaining second-order interactions of the ground and lowest excited configurations were taken into account by a standard CI treatment which includes all one- and two-electron excitations with

TABLE 4

Electric $\vec{\mu}$ (10^{-2} a.u.) and magnetic $\vec{m}$ ($10^{-2}i$ a.u.) transition dipoles rotational strengths R from CI wavefunctions (1 200 CI components)

State and local symmetry	Axes	$\vec{\mu}$	$\vec{m}$	R
$n \longrightarrow \pi^*$ (B_1)	z	−2.194	−6.343	
	y	−0.230	110.329	−2.149
	x	−47.950	1.642	
$\pi \longrightarrow \pi^*$ (L_b)	z	0.043	−0.438	
	y	8.356	7.300	1.564
	x	−2.920	−1.847	
$n \longrightarrow \pi^*$ (A_1)	z	1.665	−4.790	
	y	0.457	−0.165	0.002
	x	−2.996	−2.714	
$n \longrightarrow \pi^*$ (L_a)	z	−10.143	−5.582	
	y	0.151	−3.345	1.243
	x	3.287	−1.028	

respect to the ground and excited configurations in equations (4). Excitations were restricted to the subset of orbitals listed in Figure 2 and the resulting wave-functions were expressed as linear combinations of *ca.* 1 200 CI components.

On energy grounds, the most important effect of the CI treatment is a strong stabilization of the ^1L_b state with respect to the lowest $n \longrightarrow \pi^*$ state (see Table 6). The interaction of the $n \longrightarrow \pi^*(B_1)$ and ^1L_b states increases therefore considerably and accounts for the large increase of the magnetic transition moment to the ^1L_b state (m_y) and for the sign reversal of the electric transition dipole to the $n \longrightarrow \pi^*(B_1)$ state (μ_y) (Tables 4 and 5).

A second important effect of the CI treatment is the mixing of the $n \longrightarrow \pi^*$ configuration (5,8) with the second excited $n \longrightarrow \pi^*$ configuration with the same local symmetry (5,10). As shown in Tables 1 and 5, the (5,10) configuration, besides making important contributions to the μ_x and m_y components of the electric and

TABLE 5

Main contribution to the electric $\vec{\mu}$ (10^{-2} a.u.) and magnetic $\vec{m}$ ($10^{-2}i$ a.u.) dipole components for the lowest $n \longrightarrow \pi^*$ and $\pi \longrightarrow \pi^*$ (L_a,L_b) transitions

Excited state	Axes	$\vec{\mu}$	$\vec{m}$
$n \longrightarrow \pi^*$ (B_1)	y	2.343 (5,10)	77.856 (5,8)
		5.367 (6,9)	22.867 (5,10)
		−9.271 (7,8)	−1.837 (3,8)
	x	−34.828 (5,8)	1.187 (5,10)
		−8.231 (5,10)	
L_b	y	−64.266 (6,9)	5.636 (5,8)
		71.918 (7,8)	0.989 (6.9)
			−1.422 (7,8)
	x	−2.465 (5,8)	−3.708 (7,8)
L_a	z	38.782 (6,8)	−1.428 (1,9)
		−49.917 (7,9)	−2.003 (7,9)
		1.837 (7,10)	1.691 (7,10)

magnetic dipoles, provides the dominant contribution to m_x and determines its sign.

The rotational strength of the $n \longrightarrow \pi^*$ transition results from two major contributions ($m_x\mu_x$, $m_y\mu_y$). For a small energy separation of the $n \longrightarrow \pi^*$ and ^1L_b states, the two contributions have both negative values. When the energy separation between the ^1L_b and $n \longrightarrow \pi^*$

TABLE 6

Electric $\vec{\mu}$ (10^{-2} a.u.) and magnetic $\vec{m}$ ($10^{-2}i$ a.u.) transition dipoles and rotational strengths R (10^{-39} c.g.s.) for the lowest $n \longrightarrow \pi^*$ transition computed with different CI expansions. (a) 4, (b) 100, (c) 500, and (d) 1 200 CI components. ΔE is the energy separation between the L_b and the $n \longrightarrow \pi^*$ (B_1) states

	ΔE cm^{-1}	Axes	$\vec{\mu}$	$\vec{m}$	R
(a)	~ 10 000	z	0.442	−5.666	
		y	0.051	88.872	0.764
		x	−33.872	0.897	
(b)	9 800	z	−1.895	−6.312	−0.685
		y	0.165	104.312	
		x	−42.487	1.381	
(c)	5 950	z	−2.370	−6.458	−1.034
		y	0.090	110.932	
		x	−45.385	1.524	
(d)	1 050	z	−2.194	6.343	−2.149
		y	−0.239	110.329	
		x	−47.950	1.642	

states is increased and the interaction between the ^1L_b and the $n \longrightarrow \pi^*$ states becomes less effective, the $m_y\mu_y$ contribution becomes positive with significant reduction of the rotational strength of the $n \longrightarrow \pi^*$ transition

(Table 6). This is a possible explanation of the low intensity of the negative c.d. band on the low energy side of the spectrum. In the limit of a four configuration interaction treatment [equations (4), Tables 3 and 6] the rotational strength of the $n \longrightarrow \pi^*$ transition is reversed in contrast with the experimental c.d. spectrum.

A second factor responsible for the overestimate of the rotational strength of the $n \longrightarrow \pi^*$ transition is the relatively large electric dipole predicted for the transition (Tables 1—4).

The computed rotational strength for the ^1L_b transition (Table 4) is compatible with the measured value of the second band in the spectrum of Figure 1.

Despite some important contributions from excited configurations, the CI values of the rotational strengths of the electronic transitions to the $n \longrightarrow \pi^*$ (A_2) and ^1L_a states (Tables 4 and 5) do not differ substantially from the estimates based on the simple wavefunctions (1,4) (Tables 2 and 3). On these grounds, we assign the third positive band of the c.d. spectrum to the ^1L_a state.

The main conclusions of the analysis in Table 5, the signs and the order of magnitude of the electric dipoles and rotational strengths in Tables 2—4, are not modified when the electric dipoles are evaluated in the dipole length representation and when the size of the CI expansion is changed.

Conclusions.—After inclusion of CI, the theoretical data obtained compare favourably with the experimental c.d. and absorption spectra of (III). The calculated sequence of the transitions corresponds to the current assignments proposed for pyridine,[11] *i.e.* $n \longrightarrow \pi^*$, $\pi \longrightarrow \pi^*$, ($n \longrightarrow \pi^*$), $\pi \longrightarrow \pi^*$ from low to high energy. The calculated rotational strengths are all of the correct signs and the orders of magnitude are correct for the $\pi \longrightarrow \pi^*$ transitions but high for the $n \longrightarrow \pi^*$. However, the mutual cancellation of the $n \longrightarrow \pi^*$ and ^1L_b transition is partially responsible for the observed low intensity of the two c.d. bands.

The following points seem to be relevant: (i) the low energy $n \longrightarrow \pi^*$ transition is red-shifted relative to the first $\pi \longrightarrow \pi^*$; (ii) the contribution of the second $n \longrightarrow \pi^*$ transition is negligible; (iii) the one-electron mechanism gives a correct qualitative explanation of the optical activity of the $n \longrightarrow \pi^*$ and ^1L_b transitions; (iv) The calculations carried out on the simple 5,6,7,8-tetrahydroquinoline fragment account for the optical activity of (III). The location of the important fragments in determining the optical activity of a complex molecule seems to be a promising tool for performing good calculations in large systems.

EXPERIMENTAL

C.d. spectra were measured using a Jouan II dichrograph, and absorption spectra were measured using Unicam SP 700 and Cary 14 spectrophotometers. M.p.s are uncorrected.

3-(N-pyrrolidin-1-yl)-5α-cholestan-2-ene (II).—This had m.p. 107—110° (lit.,[12] 105—110°) and was synthesized by the procedure described in ref. 12.

5α-Cholest-2-eno[3,2-b]*pyridine* (III).—Acrolein (112 mg, 2 mmol) was added to a solution of enamine (880 mg, 2 mmol) in anhydrous benzene [13] (5 ml) at 0 °C and the solution was stirred overnight at room temperature. The solvent was removed under reduced pressure and the residue refluxed (3 h) with hydroxylamine hydrochloride [14] (417 mg, 6 mmol) in 95% ethanol (10 ml). The solution was neutralized (K_2CO_3), diluted with water and the precipitate filtered off and chromatographed on alumina (25 g).

Elution with light petroleum–diethyl ether (95 : 5) followed by two crystallizations (diethyl ether–methanol) gave pure 5α-cholest-2-eno[3,2-*b*]pyridine, homogeneous on t.l.c. [silica gel; benzene–acetone (8 : 2)], m.p. 118—118.5 °C; $[\alpha]_D^{25}$ +62.1° (*c* 0.475; absolute ethanol); δ (CCl_4; Me_4Si as internal standard) 8.25 (1 H, dd, α-H, $J_{\alpha\beta}$ 5, $J_{\alpha\gamma}$ 1.2 Hz), 7.25 (1 H, dd, γ-H, $J_{\gamma\beta}$ 8 Hz), 6.93 (1 H, dd, β-H), and 2.43 (4 H, m, 1- and 4-H); *m/e* 421 (M^+) (Found: C, 85.9; H, 11.35; N, 3.4. $C_{30}H_{47}N$ requires C, 85.45; H, 11.25; N, 3.3%).

We thank C.N.R. (Rome) for financial support.

[9/527 *Received*, 3*rd April*, 1979]

REFERENCES

[1] G. Gottarelli and B. Samorì, *Tetrahedron Letters*, 1970, 2055.
[2] G. Gottarelli and B. Samorì, *J.C.S. Perkin II*, 1972, 1998.
[3] G. Gottarelli and B. Samorì, *J.C.S. Perkin II*, 1974, 1562.
[4] H. E. Smith, L. J. Shaad, R. B. Banks, C. J. Wiant, and C. F. Jordan, *J. Amer. Chem. Soc.*, 1973, **95**, 811.
[5] Chyn-Yah Yeh and F. S. Richardson, *J.C.S. Faraday* II, 1976, 331.
[6] O. Cervinka and P. Malon, *Coll. Czech. Chem. Comm.*, 1978, **43**, 278.
[7] A. M. Manotti Lanfredi, A. Tiripicchio, and M. Tiripicchio Camellini, *Cryst. Struct. Comm.*, 1975, 153.
[8] G. Snatzke and P. C. Ho, *Tetrahedron*, 1971, **27**, 3645; G. Snatzke, M. Kajtar, and F. Werner-Zamojska, *ibid.*, 1972, **28**, 281.
[9] W. J. Hehre, R. F. Stewart, and J. A. Pople, *J. Chem. Phys.*, 1969, **51**, 2657.
[10] E. V. Condon, W. Altar, and H. Eyring, *J. Chem. Phys.*, 1937, **5**, 753.
[11] V. Olsher, *Spectrochim. Acta*, 1978, **34A**, 211.
[12] M. E. Herr and F. W. Heyl, *J. Amer. Chem. Soc.*, 1953, **75**, 1918.
[13] G. Stork, A. Brizzolara, M. Landesman, J. Szmnskovicz, and R. Terrel, *J. Amer. Chem. Soc.*, 1963, **85**, 207.
[14] C. Botteghi, G. Caccia, S. Gladiali, and D. Tatone, *Synth. Comm.*, 1979, **9**, 69.